ACS Sustainable Chemistry & Engineering

Research Article

pubs.acs.org/journal/ascecg

Biomass-Based Fuels and Activated Carbon Electrode Materials: An Integrated Approach to Green Energy Systems

Jillian L. Goldfarb,*[,†,‡] Guolan Dou,[†,§] Maryam Salari,[∥] and Mark W. Grinstaff[‡,∥,⊥]

[†]Department of Mechanical Engineering, Boston University, 110 Cummington Mall, Boston, Massachusetts 02215, United States

[‡]Division of Materials Science & Engineering, Boston University, 15 St. Mary's Street, Brookline, Massachusetts 02446, United States

[§]School of Safety Engineering, China University of Mining & Technology, No. 1 Daxue Road, Xuzhou, Jiangsu 221116, People's Republic of China

[∥]Department of Chemistry, Boston University, 590 Commonwealth Avenue, Boston, Massachusetts 02215, United States

[⊥]Department of Biomedical Engineering, Boston University, 44 Cummington Street, Boston, Massachusetts 02215, United States

Supporting Information

ABSTRACT: Although pyrolysis holds promise for extracting biofuels from biomass, the low value of the biochar produced, combined with process energy requirements, make thermochemical conversion marginally viable. Likewise, while supercapacitors and fuel cells may satisfy growing demands for portable electronics and electric vehicles, current fossil-fuel based activated carbon electrodes are not sustainable. Both of these issues are addressed using a new approach to the integrated biorefinery. Pyrolysis of pistachio nutshell biomass yields a bio-oil high in benzenediols and pyrolysis gas enriched in methane and hydrogen. By impregnating the biochars produced via pyrolysis with potassium hydroxide, followed by heat treatment in an inert atmosphere, the total biofuel yield increased up to 25% while producing high surface area (>1900 m^2/g) activated carbon biochar for use in electrochemical cells. Coin cell electrodes fabricated with these sustainable activated carbons provide almost 100% coulombic efficiency over 4000 charge−discharge cycles with a specific capacitance of 45 F/g at a scan rate of 1 mV/s using a Li-salt electrolyte. Such integrated processes will hasten the transition to a renewable energy future.

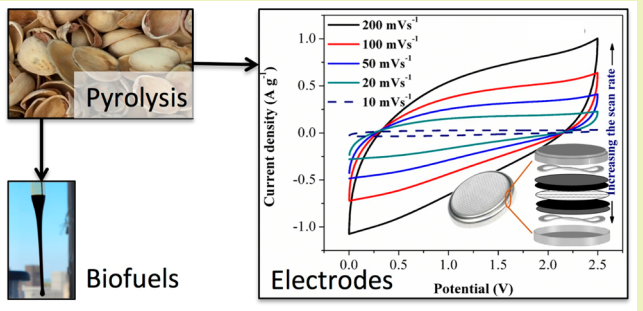

KEYWORDS: *Integrated biorefinery, Supercapacitor, Activated biochar, Green energy, Pyrolysis*

INTRODUCTION

A renewable energy future includes efficient and environmentally friendly energy production and capture, in addition to storage and use. The former will rely on, for example, solar, wind, or biomass refineries, whereas the later will utilize fuel cells, batteries, and supercapacitors prepared from sustainable materials. Biomass, i.e., organic matter, is a particularly important resource as it provides an opportunity to generate thermochemical energy and simultaneously yields a waste product useful for preparing high performance material components for electrochemical energy systems, thereby diverting these wastes from landfills and adhering to Principles of Green Engineering.[1]

Common to many electrochemical storage systems is a carbon electrode, often composed of activated carbon (AC), owing to its high surface area and porosity, efficient electrical and thermal conductivity, high stability, low economical cost, and availability.[2] Biomass-based activated carbons (activated biochars) exhibit surface areas upward of 1500 m^2/g, and are more sustainable than their fossil fuel-based counterparts.[3,4] Researchers are using these materials in a number of electrochemical devices, including lithium-ion and Li−S batteries,[5−8] supercapacitors,[9] and microbial fuel cells.[10] Biomass precursors for these activated biochars include agricultural or industrial residues such as sugar cane bagasse,[11] rice husk,[12] pits and peels of fruits,[13−15] and nutshells.[16] For example, pistachios are one significant renewable biomass of interest. More than half of a billion pounds of pistachios are produced annually in the U.S., the vast majority of which (98%) are grown in California.[45] Their shells are an inedible waste product, sold for birdcage bedding and mulch, with minimal intrinsic value.[31] However, they are high in volatile matter and fixed carbon, and relatively low in ash, representing a valuable carbon source for conversion to activated biochars.

In response to the rapidly expanding market for portable electronic devices and electric vehicles, supercapacitors (ultracapacitors) are extensively investigated due to their pulse power supply, long cycle life, and high charge propagation.[17] Based on the composition of the supercapacitor, supercapacitors are divided into three groups: nonfaradic supercapacitors (namely

Received: November 11, 2016
Revised: January 18, 2017
Published: March 8, 2017

DOI: 10.1021/acssuschemeng.6b02735
ACS Sustainable Chem. Eng. 2017, 5, 3046−3054

electric double layer capacitors; ELDCs), pseudocapacitors (faradic mechanism), as well as hybrid supercapacitors, a combination of the two former designs. Generally, carbon electrodes such as graphene, carbon nanotubes, carbon aerogels, and activated carbons are used in nonfaradic supercapacitors, whereas pseudocapacitors utilize transition metals, which lead to faradic energy storage processes and enhanced energy density. Activated carbon (AC) electrodes are commonly prepared by treating the carbon source with potassium hydroxide (KOH) to afford well-defined micropores, high micropore volumes, and high specific surface area materials.[18] Substantial efforts are also dedicated to hybrid electrochemical cells, taking advantage of both aforementioned charge storage mechanisms to fabricate supercapacitors with enhanced energy and power densities.[19−22]

Although the conversion of biomass to ACs for supercapacitors has been studied,[23−29] integrated concepts that address both renewable biofuels and sustainable ACs are of significant interest and conspicuously absent from the literature. As shown in Figure 1, an integrated biorefinery concept is

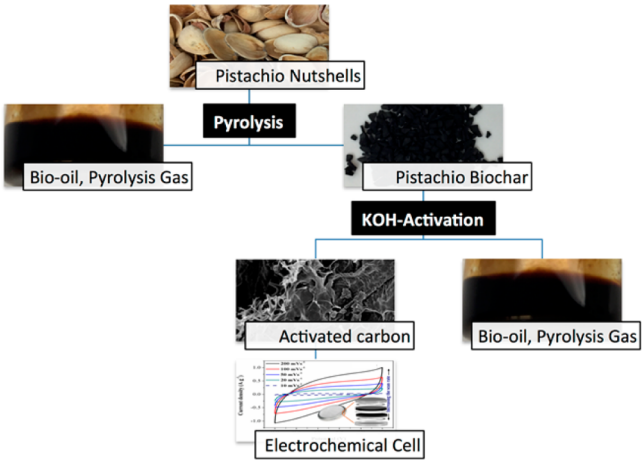

Figure 1. Proposed integrated process pathway for production of biofuels and electrochemical cell components from KOH-activation of biomass (i.e., activated biochars).

proposed whereby a raw biomass is first pyrolyzed to produce biochar, a precursor to ACs, with concurrent recovery of bio-oil and pyrolysis gas to supply energy to the process. The biochar is then chemically treated with KOH, followed by thermal activation, where a second stream of pyrolysis gas and bio-oil are collected during the production of activated biochars. The resulting biochars are available for use as electrodes in energy storage solutions. In this work using pistachio nutshell biomass, we report: (1) impact of KOH activation on biofuel composition; (2) thermochemical conversion kinetics of the biofuel process; (3) characterization of the biochars; (4) fabrication of hybrid Li-ion supercapacitor using activated biochars; and (5) electrochemical testing and supercapacitor performance evaluation. The transition from a fossil-fuel-powered society to a renewable and sustainable energy future requires design processes that integrate production of green energy along with sustainable materials for energy generation and storage.

MATERIALS AND METHODS

An optimal sustainable process that relies on biomass as a raw material neither competes with food supply or arable land for agriculture, nor increases the water necessary for cultivation.[30]

Preparation and Characterization of Raw Pistachio Nutshells. Unsalted pistachios (Wonderful Pistachios Brand) were purchased at a local grocery store and the shells and nutmeats were separated. The shells were ground in a planetary ball mill and sieved to a particle size fraction of 125−300 μm. Ultimate analysis was carried out by LECO Analytical using an elemental analyzer. Proximate analysis was performed in-house on a Mettler Toledo TGA/DSC-1 using approximately 10 mg of sample, in triplicate. Samples were loaded into 70 μL alumina crucibles. Moisture content was determined as the loss upon heating to and holding at 110 °C. The sample was then heated to 910 °C at 100 °C/min under 50 mL/min high purity nitrogen and held for 30 min; this mass loss is attributed to volatile matter. The sample was then heated at 100 °C/min up to 950 °C under air and held for 30 min to determine fixed carbon; the remaining sample mass was attributed to ash. A baseline run of an empty crucible was used to account for buoyancy effects. The higher heating value of pistachio nutshell samples was measured in-house using a Parr oxygen bomb calorimeter (calibrated with NIST-traceable benzoic acid) in triplicate. Results of these raw sample characterizations are provided in Table 1 as average of three measurements with corresponding standard deviations.

Table 1. Ultimate, Proximate and Combustion Analysis of Raw Unsalted Pistachio Nutshells

unsalted pistachio nutshells	
proximate analysis (wt %, dry basis)	
moisture (as rec'd)	5.8 ± 0.8
volatile matter	84.9 ± 1.2
fixed carbon	12.9 ± 0.7
ash	2.2 ± 0.9
ultimate analysis (wt %%, dry basis)	
C	49.2 ± 1.1
H	7.0 ± 0.3
N	0.4 ± 0.2
O	43.4 ± 1.1
higher heating value (MJ/kg)	18.02 ± 0.34

Production of Biofuels and Activated Biochars from Pistachio Nutshells. Because direct chemical activation of raw biomass often results in a low yield of powdery sample with little structural integrity,[32] the biomass is first pyrolyzed to concentrate the carbon by removing some volatiles[33,34] Ground and sieved pistachio nutshells were pyrolyzed in a porcelain boat in a tube furnace. The tube was flushed with high purity nitrogen gas for 5 min; N_2 was used throughout heat treatments at a flow rate of 100 mL/min. The samples were heated at 10 °C/min to 110 °C, held for 10 min (to drive off moisture), then pyrolyzed at 10 °C/min up to 450 °C for 45 min, and cooled under nitrogen to yield a pistachio nutshell biochar. To activate these biochars, 50 mL of a 2.5 M potassium hydroxide (Fisher Scientific, >99% purity) solution was added to 3.5 g of the pyrolyzed char (representing a 1:2 char:KOH ratio) and stirred for 1 h. The mixture was dried in an oven at 110 °C overnight, then placed in the tube furnace. The temperature was programmed to heat at 10 °C/min to 110 °C, held 10 min (to remove excess surface moisture), to 300 °C at 10 °C/min and held for 1 h to prevent steam activation upon further heating.[33,35] Finally, the sample was heated at 10 °C/min to 450 °C and held for 45 min. It is thought that the activation of carbonaceous sources with KOH proceeds via the overall reaction:

$6KOH + 2C \rightarrow 2K + 3H_2 + 2K_2CO_3$ where K_2CO_3 forms at 400 °C, with complete consumption of KOH up to 600 °C.[36] To ensure activation of the sample, while keeping the temperature as low as possible (to improve overall process energy consumption), we used an activation temperature of 450 °C. The samples were cooled to room

DOI: 10.1021/acssuschemeng.6b02735
ACS Sustainable Chem. Eng. 2017, 5, 3046−3054

temperature under nitrogen to prevent oxidation. Following this activation, the blackened chars were neutralized by adding them to 120 mL of a 0.1 M HCl solution (EMD Chemicals) and stirred for 1 h. The samples were rinsed with hot DI water until the wash water reached a pH of 6.[34] Samples were dried in the oven overnight and stored in an airtight container until further use (i.e., activated biochar).

During both the initial pyrolysis to produce a biochar, and the KOH-thermal activation, we monitored evolved gas using a Quadrupole Mass Spectrometer (Extorr XT Series RGA XT300M) at AMU signals of 2, 16, and 18 (H_2, CH_4 and H_2O, respectively). To gauge the impact of KOH activation on liquid bio-oil production, condensable gases were collected in 5 mL of dichromethane (ACROS Organics, >99.5% purity) in a cold trap. The condensable fuel components were analyzed using an Agilent 5800 gas chromatography−mass spectrometry (GC−MS) instrument. Analysis was performed in split mode with a split ratio of 5:1, with an injection temperature of 250 °C using ultra high purity helium as a carrier gas. GC conditions began with an initial oven temperature of 50 °C with a hold time of 3 min, followed by heating at 10 °C/min to 100 °C, then 15 °C/min to 180 °C, and then 20 °C/min to 300 °C with a final hold time of 5 min. Interface temperature was set at 325 °C. A semiquantitative analysis was performed by integrating the top (by area) 20 gas chromatogram peaks. Peaks are only reported if their NIST-library identification similarity was greater than 90%.

Thermochemical Conversion Kinetics of Base-Treated Pistachio Shells. We recently reported the pyrolysis kinetics and activation energies of raw pistachio shell biomass using thermogravimetric analysis.[37] As such, for this study we present data only on the KOH-activated pyrolyzed samples, to explore the impact of this chemical treatment on activation energy and thermal degradation kinetics. Conversion kinetics were determined using the Mettler-Toledo TGA/DSC-1. Samples (8−12 mg each) of KOH-soaked pistachio nutshells were heated at 10 °C/min under high purity N_2 to 110 °C and held for 30 min to remove water. They were then heated at 10, 20, or 50 °C/min up to 900 °C and held for 60 min (to ensure removal of all volatiles). Activation energy experiments were performed in accordance with Recommendations put forth by the ICTAC Kinetics Committee, who suggested use of isoconversional methods with at least three temperatures to overcome heating rate as an experimental variable.[38] Such methods often rely on the Arrhenius equation, given as

$$k = A\mathrm{e}^{-E/RT} \tag{1}$$

where k is the reaction rate constant, A is the pre-exponential (or frequency) factor, E the activation energy, T is absolute temperature, and R the universal gas constant. Using the Mettler Toledo TGA-DSC-1, we collected nonisothermal TGA data at a series of heating rates, $\beta = \mathrm{d}T/\mathrm{d}t$, Data were transformed to arrive at an extent of conversion, $X(t)$, as a function of initial mass, m_i, final mass, m_f, and mass at any time t, m_t:

$$X(t) = \frac{m_\mathrm{i} - m_t}{m_\mathrm{i} - m_\mathrm{f}} \tag{2}$$

Like many isoconversional methods used to describe pyrolysis reaction kinetics, the Distributed Activation Energy Model (DAEM) assumes that countless irreversible first order parallel reactions occur simultaneously, each with its own activation energy.[39,40] The combined reactions are represented by a distribution function, $f(E)$, which when taken over several constant temperature ramp rates, assumes the form:[41]

$$X(t) = 1 - \int_0^\infty \exp\left(-\frac{A}{\beta}\int_0^t \exp\left(-\frac{E}{RT}\right)\mathrm{d}T\right) f(E)\mathrm{d}E \tag{3}$$

It is commonly assumed that the function, $f(E)$, is normally distributed with average activation energy, E_a and a standard deviation, σ:

$$f(E) = \frac{1}{\sigma\sqrt{2\pi}}\exp\left[-\frac{(E - E_\mathrm{a})^2}{2\sigma^2}\right] \tag{4}$$

Non-Gaussian distributions are sometimes used to represent $f(E)$, including Weibull, Gamma, and Maxwell−Boltzmann distributions.[42−44] Some incarnations of the DAEM consider the frequency factor a constant for all reactions; the Integral method proposed by Miura and Maki[45] allows for a compensation effect between A and E. As the pre-exponential factor represents both the collision frequency of molecules during a chemical reaction, and the success of these collisions between those molecules to result in a reaction, it follows to reason that this factor depends on the number of molecules present in a control volume. Furthermore, because the number of molecules participating in thermal decomposition reactions increase with temperature, and yet decrease as volatiles are lost from the solid, we applied the Integral Method to account for the dynamic nature of the pre-exponential factor across the range of mass fraction conversions.

Characterization of Activated Pistachio Shell Biochars. The carbon content of the activated material was determined using TGA. The surface area and pore volume were measured using an ASAP 2020 Surface Area Analyzer (Micromeritics, Norcross, GA) using ultra high purity nitrogen adsorption isotherms at 77 K. Approximately 0.30 g of sample was used, measured on a Sartorius semimicrobalance accurate to 10^{-4} grams. The sample was degassed under vacuum at 120 °C for 5 h. After degassing, the sample was maintained at room temperature, under vacuum, before analysis. Immediately upon removing the sample from the degasser, it was reweighed and loaded for analysis. The specific surface areas of samples were estimated using the BET theory in the partial pressure range of 0.05 to 0.30 and total pore volume over the entire partial pressure range.

Fabrication of Coin Cell Electrodes. To prepare working electrodes, 75 wt % of the activated biochar prepared from the pistachio nutshells and 15 wt % carbon black (MTI Co.) were mixed with 10 wt % poly(vinylidene fluoride) (PVDF, Sigma-Aldrich) binder in a mortar. A uniform slurry was formed by adding a few drops of *N*-methylpyrrolidinone (NMP) solvent. The slurry was distributed on a previously punched and washed titanium substrate of 1.58 cm in diameter, followed by drying in a vacuum oven at 80 °C for 12 h. Two identical electrodes (by mass) separated by a filter paper (Whatman) were used to assemble the CR2032 coin cell (MTI Co.) supercapacitors in an argon-filled glovebox. Stainless steel foils and 1 M lithium bis(trifluoromethanesulfonyl) imide (LiTFSI) dissolved in propylene carbonate (PC) were used as current collector and electrolyte, respectively. The configuration of the activated biochar//PC: LiTFSI-1M//AC supercapacitor coin cell was set using a punch cell machine (MTI Co.)

Electrochemical Testing. Cyclic voltammetry (CV) and charge−discharge (CD) tests were preformed using a Princeton Applied Research VersaStat battery tester. Electrochemical measurements were conducted over a voltage range of 0 to 2.5 V at various scan rates (from 1 to 200 mV s^{-1}) and different current densities (from 0.5 to 5 A g^{-1}) at room temperature. All the calculations are based on the total mass of the active materials. The specific capacitance of the working electrode in the coin cell configuration was calculated by integrating the area under the CV or CD curves using eq 5 or eq 6, respectively.

$$C_\mathrm{s} = 2I\frac{\mathrm{d}V}{\mathrm{d}t}m \tag{5}$$

where, C_s is the specific capacitance (F g^{-1}), I is the charge−discharge current (A), $\mathrm{d}v/\mathrm{d}t$ is the scan rate (V s^{-1}), and m is the mass (g) of active materials.

$$C_\mathrm{s} = 4\frac{I_\mathrm{const}}{m\frac{\mathrm{d}v}{\mathrm{d}t}} \tag{6}$$

where, I_{const} is the constant current, and $\mathrm{d}v/\mathrm{d}t$ is (also equal to) the slope of the charge or discharge curve.

The coulombic efficiency, η (%), was calculated as

$$\eta\ (\%) = C_\mathrm{discharge}/C_\mathrm{charge} \tag{7}$$

DOI: 10.1021/acssuschemeng.6b02735
ACS Sustainable Chem. Eng. 2017, 5, 3046−3054

RESULTS AND DISCUSSION

To demonstrate the proposed integrated concept for renewable energy and material production, we present an integrated biorefinery concept that produces KOH-activated carbons (activated biochars) for use in supercapacitors while simultaneously capturing liquid and gaseous biofuels.

Impact of KOH Activation on Resulting Biofuels and Activated Biochars. Although there are myriad studies that probe the thermochemical conversion of biomass to biofuels, few consider how to employ the solid biochar remaining after pyrolysis beyond immediate uses such as soil amendments or sorbents for water treatment. A handful of studies describe the thermochemical conversion of pistachio nutshells to biofuels, and for information on the yields, the ability to tune product distribution as a function of pyrolysis temperature, heating rate, and other process variables, see the publications by Pütün et al.,[46] Okutucu et al.,[47] and Açıkalın et al.[48] However, none of these studies consider the possibility of a secondary biofuel extraction during the up-conversion of the solid biochar remaining after pyrolysis, nor do they demonstrate an integrated concept such as that proposed here whereby a single biomass source could yield both liquid fuels and materials for energy storage. In the present study, the pyrolysis products and conversion kinetics of raw pistachio nutshells are considered alongside those resulting from a secondary KOH-activation step of the nutshells to determine the feasibility of further extracting renewable fuels during the activation of biochars.

In Table 2, the results from a Distributed Activation Energy Model analysis show that an average activation energy for the KOH-treated shells heated to 450 °C (75.4 ± 20.4 kJ/mol) is almost half of the value measured for the pyrolysis of raw pistachio shells (149.9 ± 10.7 kJ/mol),[37] suggesting that the KOH acts as a catalyst, as well as a porogen, especially given that the more volatile compounds are removed during the initial pyrolysis step. As shown in Figure 2, the rate of decomposition is an order of magnitude lower for the activated biochar as compared to the raw sample at each heating rate, though the total sample devolatilized for the actviated biochar is also considerably lower; the char yield of raw pistachio pyrolysis is between 20 and 25 wt %, and for KOH-heating is ∼50 wt % (leading to an overall activated biochar yield of ∼10−12 wt % for the entire process.) It is well-known that the yield for pyrolysis gas for pistachio nutshells is a function of pyrolysis temperature and heating rate; at the conditions used here, the gas yields are approximately 20 wt % of the starting solid.[46−48] Methane and hydrogen steadily evolve over the pyrolysis process at 400 °C with 4.71 ± 0.24 mL of and 4.32 ± 0.22 mL, respectively, of gas per gram of raw pistachio shells (Figure 3). Interestingly, an additional 1.90 ± 0.10 mL and 1.26 ± 0.06 mL of CH_4 and H_2, respectively, per gram are obtained with the pyrolysis of activated biochar, demonstrating an increase in pyrolysis gas yield by ∼30% due to the activation process.

Yields of the oil phase from pistachio nutshell pyrolysis range from 20 to 30 wt % of the raw solid.[46−49] Though we do not have the ability to quantify the volume of liquid released, GC−MS characterization shows similar compounds evolved (primarily phenols, pyrazine, and diols) to literature results. Similar compounds also evolved during pyrolysis of the raw nutshells as during the activation step, though as shown in Figure 3, the total ion counts are approximately 50% lower for the activated compound collection. To enable detection of compounds, the condensed components from pyrolysis of the activated sample were concentrated twice (as compared to the raw sample), suggesting the ability to increase total bio-oil yield by an additional ∼25% during the activation procedure.

Table 2. Thermal and Biofuel Product Analysis of Raw and KOH-Treated Pistachio Shells Pyrolyzed at 10°C/min (with 95% confidence intervals)

		raw pistachio shells	KOH-treated pistachio shells
thermal analysis			
carbon content (wt. fraction)		0.826 ± 0.32	0.957 ± 0.25
average activation energy (kJ/mol)*		149.9 ± 10.7	75.4 ± 20.4
surface area and porosity analysis			
BET surface area (m^2/g)		2.2 ± 1.5	1971 ± 59
total pore volume (cm^3/g)			0.774 ± 0.012
pyrolysis gas analysis			
		volume evolved per gram sample (mL gas/g sample)	
	methane	4.71 ± 0.24	1.90 ± 0.10
	hydrogen	4.32 ± 0.22	1.26 ± 0.06
bio-oil analysis			
retention time (min)	component	percent area top 10 species chromatogram	
6.63	phenol, 4-ethyl-2-methyl-	16.8% ± 1.0%	14.7% ± 0.9%
6.84	1,2-benzenediol, 3-methoxy-	2.7% ± 0.5%	
6.96	benzeneethanol, 2-methoxy-		8.1% ± 0.7%
7.01	pyrazine	11.4% ± 0.8%	8.6% ± 0.7%
7.25	4-methyl-1,2-benzenediol	6.5% ± 0.7%	
7.58	2-methoxy-4-vinylphenol	4.1% ± 0.6%	
9.12	4-dimethyl-3-(methoxycarbonyl)-5-ethylfuran	14.8% ± 0.9%	8.7% ± 0.7%

[a]Samples pyrolyzed at 10, 20, and 50 °C/min for isoconversional kinetics analysis.

One of the key factors in choosing an efficient electrode material is obtaining a high surface area and thin pore walls, to reduce mass transport limitations of the electrolyte and enable enhanced ion transport, respectively. Qualitatively, treatment with KOH produces a porous activated biochar as shown in the micrographs (Supporting Information Figure S2). Quantitatively, the BET surface area (SA) of the KOH-activated pistachio nutshells is 1971 ± 59 m^2/g, and its total pore volume, V_{total}, of 0.774 ± 0.012 cm^3/g, is composed of over 99% micropores. The average pore diameter is 1.57 nm (calculated as $4 \times V_{total}/SA_{BET}$). The activated biochar material is composed of 95.7 ± 2.5 wt % carbon. These characteristics are in line with other activated biochars/carbons produced from pistachio nutshells in the literature. For example, Hassan et al.,[49] using a much larger initial particle size (1−2 mm), produced materials with SA = 1218 m^2/g and V_{total} = 0.772 cm^3/g using a 2:1 KOH:char ratio, and an activation temperature of 750 °C. The presently demonstrated process uses a considerably lower activation temperature (300 °C lower) to achieve a higher surface area and equal pore volume to Hassan et al.'s work, "greening" the process in terms of overall energy requirements. Future work will explore optimal activation temperatures as a function of surface area and electrochemical performance.

KOH-Activated Pistachio Nutshell Carbons as Electrode Materials. Cyclic voltammetry enables investigation of the electrochemical properties and capacitance response of the

DOI: 10.1021/acssuschemeng.6b02735
ACS Sustainable Chem. Eng. 2017, 5, 3046−3054

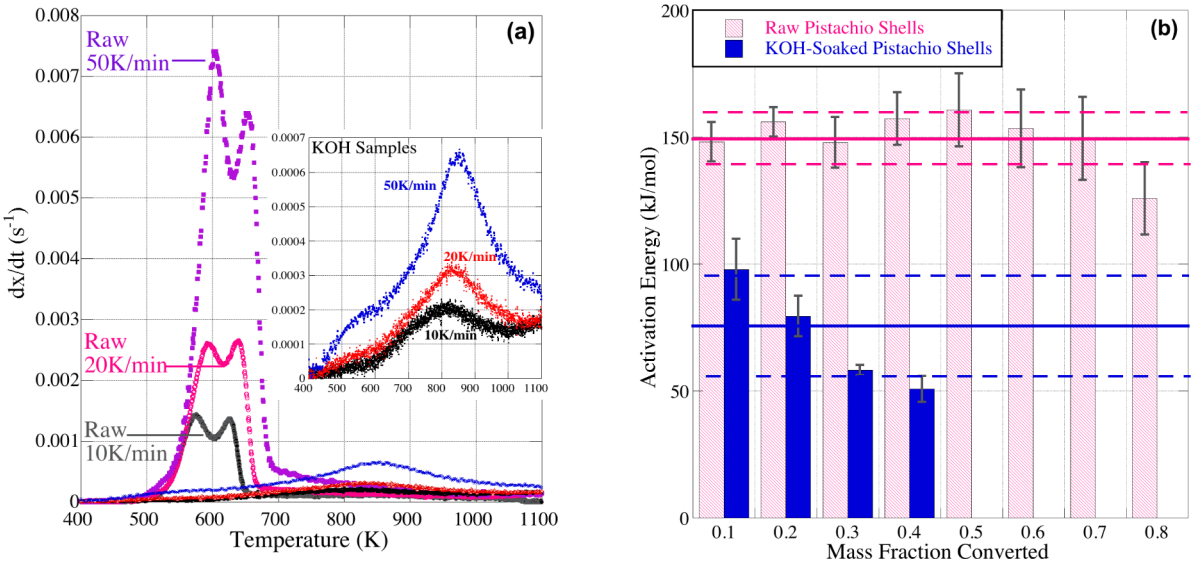

Figure 2. Thermal analysis of pyrolysis of raw and activated pistachio shells. (a) Derivative thermogravimetric curves for raw and KOH-activated pistachio shells pyrolyzed at 10, 20, and 50 K/min (inset magnifies KOH samples). (b) Activation energies of pyrolysis for raw and KOH-soaked pistachio shells at 10 wt % conversions from 0.1 to 0.8 (raw) and 0.1 to 0.3 (KOH); error bars indicate ± one standard deviation; horizontal lines indicates average E_a ± 1 standard deviation).

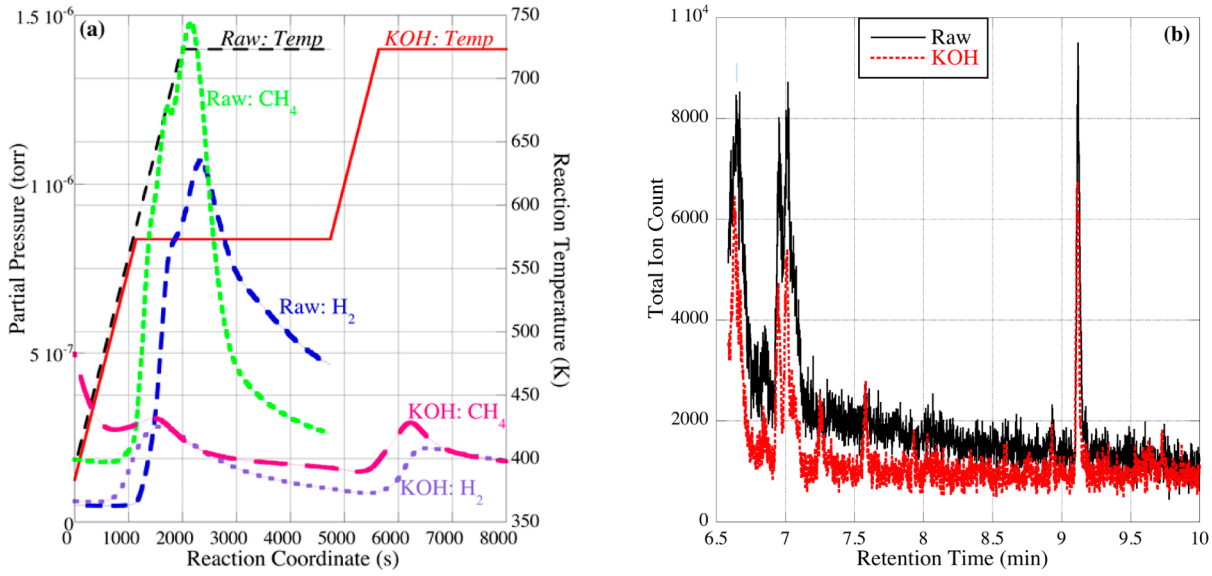

Figure 3. Analysis of H_2 and CH_4 evolved in pyrolysis gas (a) and liquid (b) biofuels produced from raw pistachio nutshells and activated biochars. (a) Pyrolysis gas evolved and monitored by MS during pyrolysis. (b) Bio-oil condensed in dichloromethane and analyzed by GC−MS after pyrolysis.

electrode materials. CV curves for the activated biochars, obtained at scan rates of 200 mV s^{-1} down to 1 mV s^{-1}, are shown in Figure 4a. The recorded CV curves slightly deviate from the ideal behavior of an electric double-layer capacitor (EDLC), which follows a rectangular path over the charge and discharge process, resulting in a mirror current response with respect to the baseline.[20] This result indicates existence of charge transference between the electrode and electrolyte. Specifically, it is due to the Li intercalation into the AC porous layers upon using a Li-salt in the electrolyte, whereas a double layer phase is maintained on the surface of the electrode material. The gravimetric normalized capacitance of the device is calculated based on the mass of both working electrodes. The calculated specific capacitance and corresponding current density of the electrode plotted against the scan rate are shown in Figure 4b. The activated biochar cell exhibits a specific capacitance of 45 F g^{-1} at a scan rate of 1 mV s^{-1}, which is similar to cells fabricated from $ZnCl_2$-activated coffee shells and orange peel in KOH electrolyte.[50,51] A range of specific capacitance values from 28 to 156 F/g are reported in the literature for activated carbon-based electrodes in supercapacitors (a survey of these values is available in Table S2 of Supporting Information). Not surprisingly, the capacitance drops by increasing the scan rate, which is a direct result of the charge transference limitation at higher sweep rates.[52] However, the activated biochar carbon electrode material maintained a capacitance of 6 F g^{-1} at a scan rate of 200 mV s^{-1}. This relatively high capacitance is attributed to the highly porous architectures of the active materials facilitating the ionic mass

DOI: 10.1021/acssuschemeng.6b02735
ACS Sustainable Chem. Eng. 2017, 5, 3046−3054

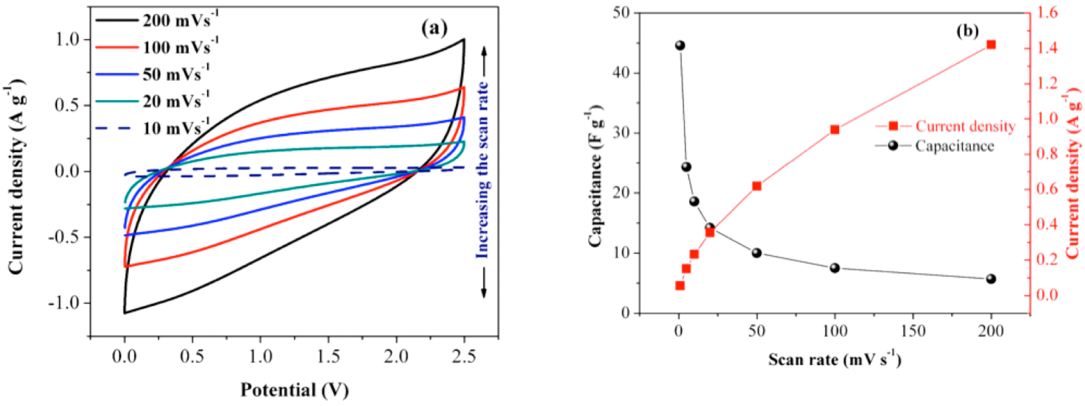

Figure 4. CV studies for the supercapacitor in PC electrolyte. (a) CV curves at various scan rates. (b) Calculated capacitance and corresponding current density gained at different scan rates.

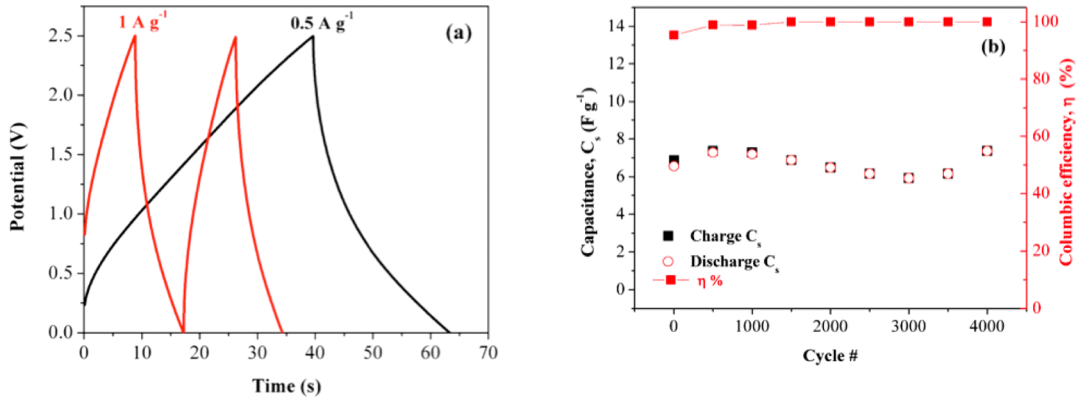

Figure 5. Charge−discharge studies for the supercapacitor in PC electrolyte. (a) CD curves obtained at low and high applied current densities. (b) Charge and discharge capacitance retention along with coulombic efficiency for 4000 cycles at a current density of 1 A g^{-1}, exhibiting nearly 100% coulombic efficiency over 4000 charge−discharge performance.

transfer and the dynamic sheath of solvent molecules through the carbon layers and porous channels.[20]

Galvanostatic charge−discharge (CD) tests were performed to evaluate the charging mechanism in the electrochemical cells. The CDs carried out at current densities of 0.5 and 1 A g^{-1} over the same potential window used in the CV investigations are shown in Figure 5a. The specific capacitance is 10 F g^{-1} with a current density of 0.5 A g^{-1}, and this result is in good agreement with the CV findings. The charge−discharge curves deviate from a linear relationship particularly at a current density of 0.5 A g^{-1}. This is due to the facilitated Li-ion intercalation at lower applied current densities. Even though no distinct redox reaction were observed in CD or CV tests, respectively, it is presumed that the Li intercalation partially contributes to the charge storage mechanism, resulting in a nonfaradic mechanism owing to utilization of a Li-salt in the electrolyte.

The capacitance retention of the supercapacitor device at a constant applied current density of 1 A g^{-1} as a function of cycle number is shown in Figure 5b. A fairly stable charge and discharge capacitance, with approximately 100% coulombic efficiency at the end of 4000 cycles, is observed. Even though there is no dramatic change in the capacitance retention over the extended course of the charging process, the slight capacitance fluctuation might be due to the solid-electrolyte interphase (SEI) layer formation. It is well established that formation of SEI (from the Li salt dissolved in the electolyte) protects the electrolyte and electrode from further reduction and degradation. SEI layers usually form at the first cycles of the charging process and have a post effect on the cell longevity. However, prolonged cycling at various conditions results in degradation of the SEI layer, leading to alteration of the internal charge resistance and poorer performance of the cells. Because the trend in the charge and discharge capacitance is fairly constant with nearly 100% coulombic efficiency over the long-term CD procedure, it is likely that the capacitance fluctuation is due to the degradation and reformation of SEI layers.

Integrated Approach to Converting Biomass to Green Energy. While the pistachio activated biochar capacitors fabricated in the present work are on the lower end of published specific capacitance values (ranging from 28 to 156 F/g), the present study uses a different electrolyte and current collector (as materials were available in-house) than other studies. The results shown in Figure 6 underscore how surface area and pore volume cannot be the only variables impacting specific capacitance of activated-based electrodes; activated carbons with surface areas as low as 528 m^2/g displayed specific capacitance values ranging from 41 to 78 F/g[52] and materials with surface areas as high as 2371 m^2/g have specific capacitance values as low as 28 F/g.[53] Factors such as the activated carbon's surface functional groups, pore size distribution, as well as electrolyte and current collector all influence the resulting electrochemical cell performance. However, data across the literature show the potential for using low-cost, biomass-based activated biochars as electrodes for supercapacitors and other electrochemical applications. This

DOI: 10.1021/acssuschemeng.6b02735
ACS Sustainable Chem. Eng. 2017, 5, 3046−3054

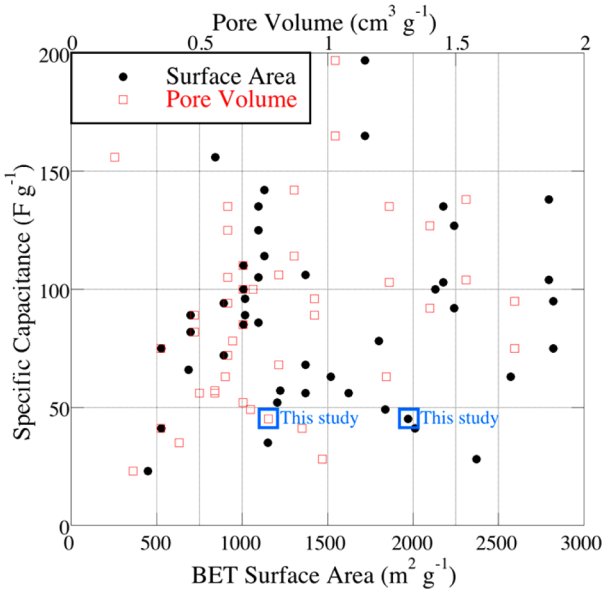

Figure 6. Specific capacitance as a function of BET surface area (●) and pore volume (□) for literature examples of activated-carbon supercapacitor electrodes (data compiled for this figure available in the Supporting Information).

paper demonstrates that it is possible to increase the bio-oil yield (by up to 25%) and gas yield (up to 30%) of an integrated biorefinery by capturing the evolved products during heat treatment of KOH-impregnated biochars. This represents a greener approach to the production of activated carbon electrodes via the use of activated biochars for supercapacitor and other electrochemical energy storage devices in an integrated biorefinery.

CONCLUSIONS

Considering alternative materials for renewable fuel applications, the potential to use waste products as building blocks for energy generation and storage represents significant fundamental science/engineering and commercial opportunities. An integrated biorefinery concept is described whereby pyrolyzed pistachio nutshells are chemically activated using potassium hydroxide to produce a high surface area (<1900 m^2/g) activated biochar suitable for use as an electrochemical cell electrode. The uniqueness of the proposed concept includes increasing the total yield of biofuels by up to 25% above the initial pyrolysis yield by capturing the liquid and gaseous components evolved during the activation step heat treatment. Pyrolysis of the KOH-activated pistachio nutshells requires a lower activation energy (as determined by the isoconversional Distributed Activation Energy Model) than pyrolysis of the raw biomass, and the condensable fuels evolved at this stage are lower in phenolic content than the raw biomass with similar methane:hydrogen ratios. The resulting activated biochars can be used as electrode materials, as demonstrated through cyclic voltammetry studies using coin cell electrodes fabricated with lithium bis(trifluoromethanesulfonyl) imide (LiTFSI) dissolved in propylene carbonate (PC) as the electrolyte. At a scan rate of 1 mV s^{-1}, the activated biochar-based cell produces a specific capacitance of 45 F g^{-1} and maintains a capacitance of 6 F g^{-1} at a scan rate of 200 mV s^{-1}. The activated biochar electrode exhibits a relatively stable charge and discharge capacitance with almost 100% coulombic efficiency after 4000 cycles. The present work demonstrates the ability simultaneously to upgrade pyrolysis biochars and extract additional biofuels during heat treatment of KOH-activated biochars. These activated biochars are then used as electrode materials for energy storage devices, eliminating the need for fossil fuel derived activated carbons. Such an integrated approach to the production of renewable fuels and energy storage materials from waste biomass could satisfy growing global demand for portable electronic devices and electric vehicles in a more sustainable, environmentally friendly way.

ASSOCIATED CONTENT

Supporting Information

The Supporting Information is available free of charge on the ACS Publications website at DOI: 10.1021/acssuschemeng.6b02735.

Kinetics analysis, compilation of literature data on activated carbon electrode materials (PDF)

AUTHOR INFORMATION

Corresponding Author

*J. L. Goldfarb. E-mail: jilliang@bu.edu; JillianLGoldfarb@gmail.com. Tel.: (617) 353 3883.

ORCID

Jillian L. Goldfarb: 0000-0001-8682-9714

Mark W. Grinstaff: 0000-0002-5453-3668

Notes

The authors declare no competing financial interest.

ACKNOWLEDGMENTS

A portion of this material is based upon work supported by the National Science Foundation under Grant No. NSF CBET-1127774. G. Dou acknowledges support of the China Scholarship Council (CSC) under Grant CSC No. 201506425012.

REFERENCES

(1) Anastas, P. T.; Zimmerman, J. B. Peer Reviewed: Design Through the 12 Principles of Green Engineering. *Environ. Sci. Technol.* **2003**, *37* (5), 94A−101A.

(2) Pandolfo, A.; Hollenkamp, A. Carbon Properties and Their Role in Supercapacitors. *J. Power Sources* **2006**, *157* (1), 11−27.

(3) Carrott, P.; Carrott, M. Lignin−From Natural Adsorbent to Activated Carbon: A Review. *Bioresour. Technol.* **2007**, *98* (12), 2301−2312.

(4) González, A.; Plaza, M.; Rubiera, F.; Pevida, C. Sustainable Biomass-Based Carbon Adsorbents for Post-Combustion CO 2 Capture. *Chem. Eng. J.* **2013**, *230*, 456−465.

(5) Arrebola, J.; Caballero, A.; Hernán, L.; Morales, J.; Olivares-Marín, M.; Gómez-Serrano, V. Improving the Performance of Biomass-Derived Carbons in Li-Ion Batteries by Controlling the Lithium Insertion Process. *J. Electrochem. Soc.* **2010**, *157* (7), A791−A797.

(6) Li, J.; Qin, F.; Zhang, L.; Zhang, K.; Li, Q.; Lai, Y.; Zhang, Z.; Fang, J. Mesoporous Carbon from Biomass: One-Pot Synthesis and Application for Li−S Batteries. *J. Mater. Chem. A* **2014**, *2* (34), 13916−13922.

(7) Unur, E. Functional Nanoporous Carbons from Hydrothermally Treated Biomass for Environmental Purification. *Microporous Mesoporous Mater.* **2013**, *168*, 92−101.

(8) Unur, E.; Brutti, S.; Panero, S.; Scrosati, B. Nanoporous Carbons from Hydrothermally Treated Biomass as Anode Materials for Lithium Ion Batteries. *Microporous Mesoporous Mater.* **2013**, *174*, 25−33.

(9) Chang, J.; Gao, Z.; Wang, X.; Wu, D.; Xu, F.; Wang, X.; Guo, Y.; Jiang, K. Activated Porous Carbon Prepared from Paulownia Flower for High Performance Supercapacitor Electrodes. *Electrochim. Acta* **2015**, *157*, 290−298.
(10) Zou, L.; Qiao, Y.; Wu, Z.; Wu, X.; Xie, J.; Yu, S.-H.; Guo, J.; Li, C. M. Tailoring Unique Mesopores of Hierarchically Porous Structures for Fast Direct Electrochemistry in Microbial Fuel Cells. *Adv. Energy. Mat* **2016**, *6* (4), 1501535.
(11) Rufford, T.; Hulicova-Jurcakova, D.; Khosla, K.; Zhu, Z.; Lu, G. Q. Microstructure and Electrochemical Double-Layer Capacitance of Carbon Electrodes Prepared by Zinc Chloride Activation of Sugar Cane Bagasse. *J. Power Sources* **2010**, *195* (3), 912−918.
(12) Guo, Y.; Qi, J.; Jiang, Y.; Yang, S.; Wang, Z.; Xu, H. Performance of Electrical Double Layer Capacitors with Porous Carbons Derived from Rice Husk. *Mater. Chem. Phys.* **2003**, *80* (3), 704−709.
(13) Elmouwahidi, A.; Zapata-Benabithe, Z.; Carrasco-Marín, F.; Moreno-Castilla, C. Activated Carbons from KOH-Activation of Argan (Argania Spinosa) Seed Shells as Supercapacitor Electrodes. *Bioresour. Technol.* **2012**, *111*, 185−190.
(14) Subramanian, V.; Luo, C.; Stephan, A.; Nahm, K. S.; Thomas, S.; Wei, B. Supercapacitors from Activated Carbon Derived from Banana Fibers. *J. Phys. Chem. C* **2007**, *111* (20), 7527−7531.
(15) Ubago-Pérez, R.; Carrasco-Marín, F.; Fairén-Jiménez, D.; Moreno-Castilla, C. Granular and Monolithic Activated Carbons from KOH-Activation of Olive Stones. *Microporous Mesoporous Mater.* **2006**, *92* (1), 64−70.
(16) Wu, F.; Tseng, R.; Hu, C.; Wang, C. Effects of Pore Structure and Electrolyte on the Capacitive Characteristics of Steam-and KOH-Activated Carbons for Supercapacitors. *J. Power Sources* **2005**, *144* (1), 302−309.
(17) Zhang, L.; Zhao, X. Carbon-Based Materials as Supercapacitor Electrodes. *Chem. Soc. Rev.* **2009**, *38* (9), 2520−2531.
(18) Wang, J.; Kaskel, S. KOH Activation of Carbon-Based Materials for Energy Storage. *J. Mater. Chem.* **2012**, *22* (45), 23710−23725.
(19) Aboutalebi, S. H.; Jalili, R.; Esrafilzadeh, D.; Salari, M.; Gholamvand, Z.; Aminorroaya, S. A.; Konstantinov, K.; Shepherd, R. L.; Chen, J.; Moulton, S. E.; Innis, P. C.; Minett, A. I.; Razal, J. M.; Wallace, G. G. High-Performance Multifunctional Graphene Yarns: Toward Wearable All-Carbon Energy Storage Textiles. *ACS Nano* **2014**, *8* (3), 2456−2466.
(20) Salari, M.; Aboutalebi, S.; Konstantinov, K.; Liu, H. K. A Highly Ordered Titania Nanotube Array as a Supercapacitor Electrode. *Phys. Chem. Chem. Phys.* **2011**, *13* (11), 5038−5041.
(21) Salari, M.; Konstantinov, K.; Liu, H. Enhancement of the Capacitance in TiO 2 Nanotubes through Controlled Introduction of Oxygen Vacancies. *J. Mater. Chem.* **2011**, *21* (13), 5128−5133.
(22) Huang, P.; Lethien, C.; Pinaud, S.; Brousse, K.; Laloo, R.; Turq, V.; Respaud, M.; Demortiere, A.; Daffos, B.; Taberna, P. L.; Chaudret, B.; Gogotsi, Y.; Simon, P. On-Chip and Freestanding Elastic Carbon Films for Micro-Supercapacitors. *Science* **2016**, *351* (6274), 691−695.
(23) Peng, C.; Yan, X.; Wang, R.; Lang, J.; Ou, Y.; Xue, Q. Promising Activated Carbons Derived from Waste Tea-Leaves and Their Application in High Performance Supercapacitors Electrodes. *Electrochim. Acta* **2013**, *87*, 401−408.
(24) Wu, X.; Wen, T.; Guo, H.; Yang, S.; Wang, X.; Xu, A. Biomass-Derived Sponge-like Carbonaceous Hydrogels and Aerogels for Supercapacitors. *ACS Nano* **2013**, *7* (4), 3589−3597.
(25) Wei, L.; Sevilla, M.; Fuertes, A.; Mokaya, R.; Yushin, G. Hydrothermal Carbonization of Abundant Renewable Natural Organic Chemicals for High-Performance Supercapacitor Electrodes. *Adv. Energy Mater.* **2011**, *1* (3), 356−361.
(26) Liu, W.; Tian, K.; He, Y.; Jiang, H.; Yu, H.-Q. High-Yield Harvest of Nanofibers/mesoporous Carbon Composite by Pyrolysis of Waste Biomass and Its Application for High Durability Electrochemical Energy Storage. *Environ. Sci. Technol.* **2014**, *48* (23), 13951−13959.
(27) Qu, W.; Xu, Y.; Lu, A.; Zhang, X.; Li, W. Converting Biowaste Corncob Residue into High Value Added Porous Carbon for Supercapacitor Electrodes. *Bioresour. Technol.* **2015**, *189*, 285−291.
(28) Chen, H.; Hautier, G.; Jain, A.; Moore, C.; Kang, B.; Doe, R.; Wu, L.; Zhu, Y.; Tang, Y.; Ceder, G. Carbonophosphates: A New Family of Cathode Materials for Li-Ion Batteries Identified Computationally. *Chem. Mater.* **2012**, *24* (11), 2009−2016.
(29) Wang, H.; Li, Z.; Mitlin, D. Tailoring Biomass-Derived Carbon Nanoarchitectures for High-Performance Supercapacitors. *ChemElectroChem* **2014**, *1* (2), 332−337.
(30) United Nations. UN-Water: Water, food and energy nexus http://www.unwater.org/topics/water-food-and-energy-nexus/en/ (accessed September 28, 2016).
(31) Boriss, H.; Romero, C. Pistachios. AgMRC Agricultural Marketing Resource Center; 2015. Available from: http://www.agmrc.org/commodities-products/nuts/pistachios/ (accessed April 26, 2016).
(32) Yang, T.; Lua, A. Characteristics of Activated Carbons Prepared from Pistachio-Nut Shells by Physical Activation. *J. Colloid Interface Sci.* **2003**, *267* (2), 408−417.
(33) Tseng, R.; Tseng, S. Characterization and Use of High Surface Area Activated Carbons Prepared from Cane Pith for Liquid-Phase Adsorption. *J. Hazard. Mater.* **2006**, *136* (3), 671−680.
(34) Tseng, R.; Tseng, S.; Wu, F.; Hu, C.; Wang, C.-C. Effects of Micropore Development on the Physicochemical Properties of KOH-Activated Carbons. *J. Chin. Inst. Chem. Eng.* **2008**, *39* (1), 37−47.
(35) Otowa, T.; Nojima, Y.; Miyazaki, T. Development of KOH Activated High Surface Area Carbon and Its Application to Drinking Water Purification. *Carbon* **1997**, *35* (9), 1315−1319.
(36) Linares-Solano, A.; Lillo-Ródenas, M. NaOH and KOH for Preparing Activated Carbons Used in Energy and Environmental Applications. *J. Energy, Environ. Econom.* **2012**, *20* (4), 335.
(37) Işıtan, S.; Ceylan, S.; Topcu, Y.; Hintz, C.; Tefft, J.; Chellappa, T.; Guo, J.; Goldfarb, J. L. Product Quality Optimization in an Integrated Biorefinery: Conversion of Pistachio Nutshell Biomass to Biofuels and Activated Biochars via Pyrolysis. *Energy Convers. Manage.* **2016**, *127*, 576−588.
(38) Vyazovkin, S.; Chrissafis, K.; Di Lorenzo, M.; Koga, N.; Pijolat, M.; Roduit, B.; Sbirrazzuoli, N.; Suñol, J. J. ICTAC Kinetics Committee Recommendations for Collecting Experimental Thermal Analysis Data for Kinetic Computations. *Thermochim. Acta* **2014**, *590*, 1−23.
(39) Cai, J.; Liu, R. New Distributed Activation Energy Model: Numerical Solution and Application to Pyrolysis Kinetics of Some Types of Biomass. *Bioresour. Technol.* **2008**, *99* (8), 2795−2799.
(40) Pütün, A.; Özbay, N.; Önal, E.; Pütün, E. Fixed-Bed Pyrolysis of Cotton Stalk for Liquid and Solid Products. *Fuel Process. Technol.* **2005**, *86* (11), 1207−1219.
(41) Dawood, A.; Miura, K. Pyrolysis Kinetics of γ-Irradiated Polypropylene. *Polym. Degrad. Stab.* **2001**, *73* (2), 347−354.
(42) Cai, J.; Li, T.; Liu, R. A Critical Study of the Miura−Maki Integral Method for the Estimation of the Kinetic Parameters of the Distributed Activation Energy Model. *Bioresour. Technol.* **2011**, *102* (4), 3894−3899.
(43) Lakshmanan, C.; White, N. A New Distributed Activation Energy Model Using Weibull Distribution for the Representation of Complex Kinetics. *Energy Fuels* **1994**, *8* (6), 1158−1167.
(44) Burnham, A.; Braun, R. Global Kinetic Analysis of Complex Materials. *Energy Fuels* **1999**, *13* (1), 1−22.
(45) Miura, K.; Maki, T. A Simple Method for Estimating F (E) and K 0 (E) in the Distributed Activation Energy Model. *Energy Fuels* **1998**, *12* (5), 864−869.
(46) Pütün, A.; Özbay, N.; Varol, E. A.; Uzun, B. B.; Ates, F. Rapid and Slow Pyrolysis of Pistachio Shell: Effect of Pyrolysis Conditions on the Product Yields and Characterization of the Liquid Product. *Int. J. Energy Res.* **2007**, *31* (5), 506−514.
(47) Okutucu, C.; Duman, G.; Ucar, S.; Yasa, I.; Yanik, J. Production of Fungicidal Oil and Activated Carbon from Pistachio Shell. *J. Anal. Appl. Pyrolysis* **2011**, *91* (1), 140−146.
(48) Açıkalın, K.; Karaca, F.; Bolat, E. Pyrolysis of Pistachio Shell: Effects of Pyrolysis Conditions and Analysis of Products. *Fuel* **2012**, *95*, 169−177.

DOI: 10.1021/acssuschemeng.6b02735
ACS Sustainable Chem. Eng. 2017, 5, 3046−3054

(49) Hassan, A.; Youssef, A.; Priecel, P. Removal of Deltamethrin Insecticide over Highly Porous Activated Carbon Prepared from Pistachio Nutshells. *Carbon Lett.* **2013**, *14* (4), 234−242.
(50) Jisha, M.; Hwang, Y.; Shin, J.; Nahm, K.; Prem Kumar, T.; Karthikeyan, K.; Dhanikaivelu, N.; Kalpana, D.; Renganathan, N. G.; Stephan, A. M. Electrochemical Characterization of Supercapacitors Based on Carbons Derived from Coffee Shells. *Mater. Chem. Phys.* **2009**, *115* (1), 33−39.
(51) Arie, A.; Kristianto, H.; Lee, J. Activated Carbons from Orange Peel Waste as Supercapacitor Electrodes. *ECS Trans.* **2013**, *53* (31), 9−13.
(52) Wu, F.; Tseng, R.; Hu, C.; Wang, C. The Capacitive Characteristics of Activated Carbons—comparisons of the Activation Methods on the Pore Structure and Effects of the Pore Structure and Electrolyte on the. *J. Power Sources* **2006**, *159* (2), 1532−1542.
(53) Qu, D.; Shi, H. Studies of Activated Carbons Used in Double-Layer Capacitors. *J. Power Sources* **1998**, *74* (1), 99−107.

DOI: 10.1021/acssuschemeng.6b02735
ACS Sustainable Chem. Eng. 2017, 5, 3046−3054